Applied Catalysis B: Environmental 142–143 (2013) 472–478

Contents lists available at SciVerse ScienceDirect

Applied Catalysis B: Environmental

journal homepage: www.elsevier.com/locate/apcatb

Effect of K loadings on nitrate formation/decomposition and on NO_x storage performance of K-based NO_x storage-reduction catalysts

Do Heui Kim[a,*], Kumudu Mudiyanselage[b], János Szanyi[b], Ja Hun Kwak[b], Haiyang Zhu[b], Charles H.F. Peden[b]

[a] School of Chemical and Biological Engineering, Institute of Chemical Processes, Seoul National University, 1 Gwanak-ro, Gwanak-gu, Seoul 151-742, Republic of Korea

[b] Institute for Integrated Catalysis, Pacific Northwest National Laboratory, 902 Battelle Blvd., Richland, WA 99354, USA

ARTICLE INFO

Article history:
Received 21 December 2012
Received in revised form 6 May 2013
Accepted 23 May 2013
Available online 31 May 2013

Keywords:
NO_x storage-reduction
Potassium
FTIR
NO_2 TPD
Pt–K/γ-Al_2O_3
KNO_3

ABSTRACT

We have investigated the effect of K loadings on the formation and the decomposition of KNO_3 over K_2O/Al_2O_3, and measured NO_x storage performance of Pt–K_2O/Al_2O_3 catalysts with various potassium loadings. After NO_2 adsorption on K_2O/Al_2O_3 at room temperature, ionic and bidentate nitrates were observed by Fourier transform infra-red (FTIR) spectroscopy. The ratio of the former to the latter species increased with increasing potassium loading up to 10 wt%, and then stayed almost constant with additional K, demonstrating a clear dependence of loading on potassium nitrate formed. Although both $K_2O(10)/Al_2O_3$ and $K_2O(20)/Al_2O_3$ samples formed similar nitrate species identified by FTIR obtained after NO_2 adsorption, the latter has more thermally stable nitrate species as evidenced by FTIR and NO_2 temperature programmed desorption (TPD) results. With regard to NO_x storage-reduction performance of Pt–K_2O/Al_2O_3 samples, the temperature of maximum NO_x uptake (T_{max}) is 573 K up to a potassium loading of 10 wt%. As the potassium loading increases from 10 wt% to 20 wt%, T_{max} shifted from 573 K to 723 K. Moreover, the amount of NO uptake (38 cm^3 NO_x/gram of catalyst) at T_{max} increased more than three times, indicating that efficiency of K in storing NO_x is enhanced significantly at higher temperature, in good agreement with the NO_2 TPD and FTIR results. Thus, a combination of characterization and NO_x storage performance results demonstrates an unexpected effect of potassium loading on nitrate formation and decomposition processes; results important for developing Pt–K_2O/Al_2O_3 as potential catalysts as high temperature NO_x storage-reduction applications.

1. Introduction

Harmful nitrogen oxides (NO_x) emitted from automobile exhaust can have a significantly negative effect on the environment and on human health. Therefore, even stricter regulations on NO_x emission are being implemented in the near future. For this reason, special attention is being paid to the development of technologies that remove NO_x from fuel-efficient lean burn engines, since conventional three-way catalysts are not applicable under these conditions. NO_x storage-reduction catalysts (NSR), also known as lean NO_x traps (LNT), are one of the possible solutions to effectively remove NO_x under highly oxidizing (lean) condition [1]. NSR catalysts consist of three crucial components, which include platinum group metals (Pt or Pd), storage element (an alkali or alkaline earth oxide), and a catalyst support material (Al_2O_3, $MgAl_2O_4$ or CeO_2) [2]. In the NSR catalysts, platinum group metals promote NO oxidation to NO_2 during a lean phase of operation, which is then stored as nitrate on the storage element. Stored nitrates are subsequently reduced during a short rich period by introducing pulses of reductants. Thus, typical NSR operation cycles between these lean and rich phases.

Among alkali or alkaline earth oxides for the storage elements, K and Ba have been studied extensively. Ba has been applied for storing NO_x at moderate temperatures (523–623 K), while K has been considered for somewhat higher temperature applications (673–773 K). Due to the typically low temperature characteristics of exhaust from diesel engines, Ba has received more attention and has been commercialized. However, more recent development of lean burn gasoline engine technologies operating at higher temperatures, including gasoline direct injection (GDI), is renewing interest in K as the storage element. In particular, there have been several reports on the NO_x storage performance of Pt–K_2O/Al_2O_3 NSR catalysts with an emphasis on their high temperature properties [3–7]. Specific behavior of nitrate formation and decomposition on K-based NSR catalysts has also been described. Notably, Toops and coworkers have used *in situ* FTIR methods to follow nitrate

* Corresponding author. Tel.: +82 2 880 1633.
E-mail address: dohkim@snu.ac.kr (D.H. Kim).

0926-3373/$ – see front matter © 2013 Elsevier B.V. All rights reserved.
http://dx.doi.org/10.1016/j.apcatb.2013.05.063

formation on Pt–K/Al_2O_3 catalysts in the presence of H_2O and CO_2 [8,9]. More recently, Castoldi et al. [10] proposed the formation of two types of nitrates species (bidentate and ionic nitrates), and examined the reactivity of these species with reductants such as CO and H_2. In addition, based on FTIR results, it has been suggested that Pt sites are in proximity of potassium species, which is the origin of basicity [11]. However, it is important to note that the previous studies focused on K-based materials at a single K loading of either about 6 wt% [3,4,8] or 20 wt% [12], unlike prior work on BaO/Al_2O_3 [13–15] which has more comprehensively investigated the effects of loading on nitrate formation and decomposition processes, and on the NO_x storage performance. Indeed, our very recent results on K_2O/$MgAl_2O_4$ [16] NSR catalysts demonstrate particularly interesting loading effects on these processes. In this contribution, we prepared several K_2O/Al_2O_3 samples with different loadings of K and address the nitrate formation and decomposition mechanism for these materials after NO_2 adsorption by using a combination of FTIR, TPD. Based on the understanding of these processes on K_2O/Al_2O_3, NO_x storage-reduction activity measurements were carried out on Pt–K_2O/Al_2O_3 samples in order to investigate the effects of K loadings on intrinsic NO_x storage performance.

2. Experimental

2.1. Preparation of catalysts

The K_2O/Al_2O_3 NSR materials studied here were prepared by traditional impregnation methods. KNO_3 (Aldrich) was dissolved in de-ionized water, and the resulting solution was used to load K onto a γ-Al_2O_3 support with a surface area of 200 m^2/g (Condea) via incipient wetness. The resulting materials were dried and then calcined for 2 h in a 10% O_2/He gas flow at a high enough temperature (973 K) to completely decompose KNO_3 to K_2O (KNO_3 melts and subsequently decomposes at ~900 K). The samples we used throughout FTIR and NO_2 TPD experiments contained 2, 5, 10, 14 and 20 wt% K_2O on γ-Al_2O_3.

For preparation of Pt-containing samples, the KNO_3/Al_2O_3 samples obtained just after impregnation and drying were used. A 2nd incipient wetness process was then applied by using a $Pt(NH_3)_2(OH)_2$ (Strem) solution. These samples were dried and then calcined in 10% O_2/He gas flow up to 773 K. In this case, the calcination temperature did not reach more than 773 K to avoid Pt sintering; therefore, some of the KNO_3 remained in the calcined Pt–K/Al_2O_3 sample. However, this residual KNO_3 was fully decomposed during pretreatments used before NO_x storage experiments by introducing rich/lean pulses at 773 K, resulting in complete reduction of KNO_3 by H_2. Pt(2 wt%)–K_2O(5, 10, 14, 20 and 30 wt%)/Al_2O_3 samples were prepared and used for the performance measurements. To avoid changes in the K-containing samples due to CO_2 and H_2O in the ambient air, the catalysts (K_2O/Al_2O_3 or Pt–K_2O/Al_2O_3) were calcined no longer than a few days before each set of experiments. Change in the nature of supported K species under ambient air is a very slow process. For example, NO_x activity decreased by ~37% after air exposures for 3 months. Therefore, 1 or 2 days after calcination in a sealed vial are thought to have little impact on the sample.

2.2. Characterization of catalysts

The FTIR experiments were carried out in transmission mode using a Bruker Vertex 80 spectrometer, and IR spectra were collected at 4 cm^{-1} resolution. Each spectrum recorded was the average of 256 scans and was referenced to a background spectrum obtained from the clean (adsorbate-free) sample. The powder samples were pressed onto a high-transmittance, fine tungsten mesh that, in turn, was attached to a copper sample holder assembly mounted onto ceramic feed-throughs on a stainless steel rod. A K-type thermocouple was spot-welded to the top center of the W grid to monitor the sample temperature, and the sample was heated resistively. The IR cell was a 6-way stainless steel cube, attached to pumping and gas handling. All the IR experiments discussed here were carried out in batch mode; that is, certain precisely controlled amounts of adsorbates were introduced into the IR cell stepwise, and changes in the IR spectra were followed as a function of time and the amount of adsorbate introduced.

TPD experiments following NO_2 adsorption were performed in a fixed bed microcatalytic quartz reactor. A gas mixture of 0.5% NO_2/He (99.999% Purity, Matheson) was passed over 100 mg of freshly calcined K_2O/Al_2O_3 samples until the NO_2 levels returned to their input value (0.5%). All gas flows were metered by mass flow controllers (Brooks Co.). After saturation, the catalyst was purged with helium for 2 h to remove the physisobed NO_x species, and then the temperature was raised to 973 K at a constant rate of 10 K/min under helium flow (100 cm^3/min) while measuring the desorbed NO_x. The evolution of both NO and NO_2 during these TPD experiments were monitored with a chemiluminescence NO_x analyzer (42C, Thermo Electron Co.).

2.3. NO_x storage measurements of catalysts

NO_x storage performance was evaluated in a fixed bed quartz reactor (I.D. = 3/8″) operated under continuous lean-rich cycling, with powder samples (0.1167 g) located on a quartz frit. NO_x concentrations in the inlet and outlet gases were measured with the chemiluminescence NO_x analyzer. NO_x uptakes (in units of cm^3/g) are defined as the total amount of adsorbed NO_x until outlet NO_x levels reached 20% of the inlet concentration (i.e. 30 ppm), normalized by the weight of the sample used for these measurements. 20 sequences of 10 s rich and 50 s lean cycles were applied, and then NO_x uptake was measured during an extended lean cycle after the last short (10 s) rich cycle. Reactants consisted of a continuous flow of 5% CO_2 and 5% H_2O balanced with He, in addition to either a rich (4.25% H_2 in He) or lean (150 ppm NO and 5% O_2 in He) gas mixture. The rich or lean gas mixtures were introduced into the main gas flows just above the reactor by a 4-port valve controlled with an electric actuator (Valco Instruments). All gases were controlled independently by mass flow controllers (Brooks Instruments) and the total flow rate was 400 cm^3/min. We measured NO_x storage performance from 773 K to 523 K by 50 K decrements (e.g. 773 K, 723 K, 673 K, 623 K, 573 K and 523 K).

3. Results and discussion

3.1. IR studies of K_2O/Al_2O_3 samples after NO_2 adsorption

It is well known that the first step for NO_x storage is NO oxidation to NO_2 on Pt sites. In order to focus on the nitrate formation and decomposition mechanisms on the potassium NO_x storage element, NO_2 was used as the adsorbate on Pt-free K_2O/Al_2O_3 samples in the FTIR experiments. In addition, we can use NO_2 TPD experiments to investigate nitrate decomposition behavior of these samples as a function of temperature without complications due to Pt sintering at higher temperature (>773 K). Such approaches are well established for obtaining a fundamental understanding of nitrate formation/decomposition behavior on alkali- and alkaline earth-based NO_x storage elements.

After the adsorption of NO_2 on K_2O (x; x = 2, 5, 10 and 20 wt%)/γ-Al_2O_3 at 300 K, IR spectra were acquired to investigate the adsorbed species on the sample as a function of varying potassium loadings.

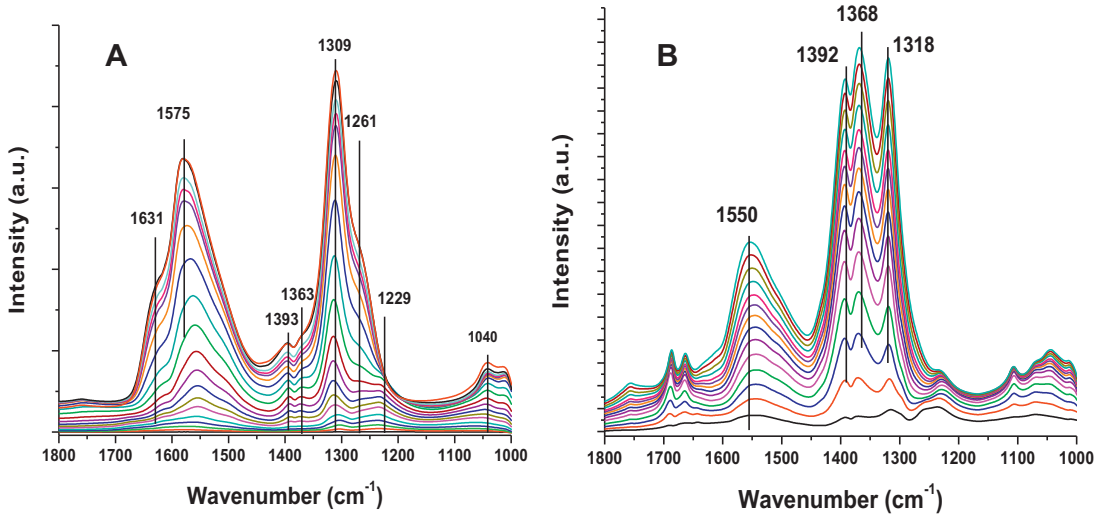

Fig. 1. FTIR spectra of (A) $K_2O(2)/Al_2O_3$ and (B) $K_2O(10)/Al_2O_3$ samples during NO_2 adsorption at room temperature.

In these experiments, NO_2 was incrementally (by 0.5 Torr) introduced into the IR cell stepwise, and an IR spectrum was taken after each dosing step until saturation; i.e., when no further changes in the spectra were evident with further NO_2 doses. The series of IR spectra obtained during stepwise NO_2 adsorption on $K_2O(2)/Al_2O_3$ and $K_2O(10)/Al_2O_3$ are illustrated in Fig. 1A and B, respectively. For the $K_2O(2)/Al_2O_3$ sample (1A), the most intense features arise from the chelating bidentate nitrates (1040, 1309 and 1575 cm^{-1}) in addition to minor peaks at 1363 and 1393 cm^{-1} which have been assigned to ionic potassium nitrates [17–19]. In addition, nitrite species are present after small doses of NO_2 as evidenced by a peak at 1229 cm^{-1}; however, its intensity diminishes rapidly with increasing amounts of NO_2. This result is similar to those reported previously [17] that primarily nitrates, both of the ionic and bidentate types, are present on Pt-free K-containing catalysts after prolonged exposure of NO_2. Note that aluminum-bound bridging bidentate nitrates are also formed at high NO_2 dosing as evidenced by the peaks at 1631 cm^{-1} and 1261 cm^{-1} [20]. This implies that aluminum sites present at low K-loadings can take part in adsorbing NO_2 to form nitrates as also seen for low-loaded Ba-containing NSR catalysts [10].

With increasing amount of potassium to 10 wt%, drastic changes were observed in the IR spectra, as displayed in Fig. 1B. In addition to the chelating bidentate nitrates (1318 cm^{-1} and 1550 cm^{-1}), ionic nitrates (1368 cm^{-1} and 1392 cm^{-1}) are also formed and grow concomitantly, resulting in the co-existence of two types of nitrate species on the NO_2-saturated sample. The results in Fig. 1 indicates that the ratio of ionic nitrates to chelating bidentate nitrates is dependent on the K loading as K loading increased from 2 wt% to 10 wt%. Again, similar phenomena have been observed in BaO/Al_2O_3 samples, where NO_2 pre-adsorbed BaO/Al_2O_3 gave rise to the two types of nitrate species (chelating bidentate nitrates and ionic nitrates) with amounts that depend on the barium loading [13]. Such dependence has been proposed to result from the preferential anchoring of barium atoms to penta-coordinated Al^{3+} sites on γ-Al_2O_3 at low Ba loading, which, correspondingly, form bidentate barium nitrates upon NO_2 adsorption [21]. For these Ba-containing NSR catalysts, particulate BaO becomes the dominant phase as Ba loading is increased to ~20 wt%, which then forms ionic barium nitrates upon NO_2 adsorption. Dependence of two types of nitrate formation upon barium loadings was comprehensively confirmed by a combination of FTIR and ^{27}Al nuclear magnetic resonance (NMR) spectroscopies, high resolution transmission electron microscopy (HR-TEM) and density functional theory (DFT) calculations [13,21,22]. Although the morphological properties of K_2O/Al_2O_3 catalysts have not been investigated as completely as BaO/Al_2O_3, based on the FTIR results in Fig. 1, we propose that highly dispersed K is formed at lower K loadings, while particulate K oxides become the major species present at higher K loadings. In support of this, note that Al-bound nitrates (at 1261 and 1631 cm^{-1}) are not observed in the $K_2O(10)/Al_2O_3$ sample (Fig. 1B), direct evidence that the Al adsorption sites are fully occupied by K atoms at this higher K loading. This conclusion is also in good agreement with the results of Montanari et al. [18], who observed similar trends in the nature of the nitrate species formed upon NO_2 adsorption to K (1, 3 and 5 wt%)/Al_2O_3 samples.

The effect of a more complete range of K loadings on the IR spectra after NO_2 adsorption to saturation coverages are presented in Fig. 2. K loading was varied from 2 wt% to 20 wt%. As K loading increases from 2 wt% to 5 wt%, there is a considerable transformation of the FTIR spectra; notably, the appearance of the two peaks at 1368 and 1395 cm^{-1} arising from ionic nitrates. For the case of Ba, the transition from bidentate to ionic nitrates was observed at barium loading between 8 wt% and 20 wt% [13]. Considering

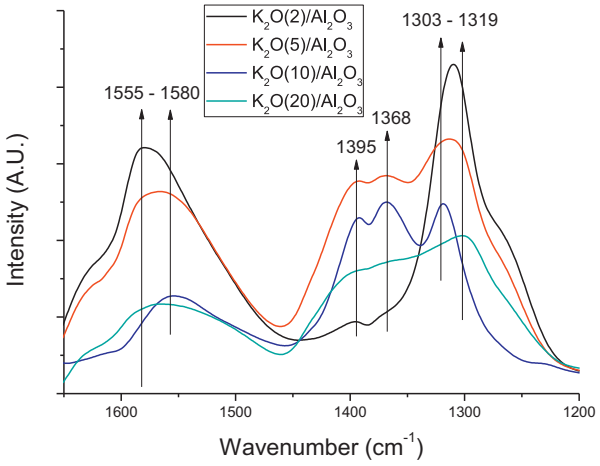

Fig. 2. FTIR spectra of NO_2 adsorbed onto $K_2O(x)/Al_2O_3$ samples with varying K_2O loadings.

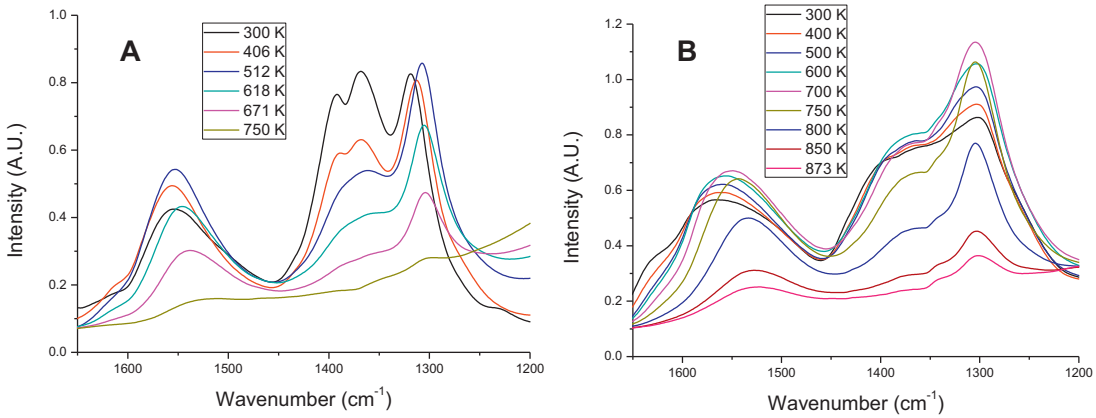

Fig. 3. FTIR spectra obtained during temperature ramping after NO_2 adsorption on (A) $K_2O(10)/Al_2O_3$ and (B) $K_2O(20)/Al_2O_3$.

that 5.4 wt% K and 16 wt% Ba loadings are equivalent molar ratios [17], it is not surprising that catalysts with higher than 5 wt% K in our study would contain mostly particulate K_2O species. Further increase in K loading from 5 wt% to 20 wt% results in a similar ratio of ionic to bidentate nitrates and, at 20 wt%, somewhat broadened IR peaks, based on a qualitative analysis of the IR peaks.

Two subsequent questions arise regarding the thermal stability of the two nitrate species formed on K_2O/Al_2O_3, as evidenced by FTIR spectra. The first one is which nitrate is more thermally stable than the other between bidentate and ionic nitrates. The second one is whether there is any difference in the thermal stability of nitrates species between K loadings of 10 wt% and 20 wt% when IR cannot readily differentiate significant differences in the nitrate species on the NO_2 adsorbed samples. The thermal decomposition behavior of the adsorbed NO_x species was investigated by obtaining FTIR spectrum during ramping to elevated temperatures.

Fig. 3A shows a series of FTIR spectra obtained from an NO_2-adsorbed $K_2O(10)/Al_2O_3$ sample during heating from 300 K to 750 K. As explained in the previous section, this sample contains two types of nitrates after adsorption of NO_2 at 300 K. When the temperature rises to 406 K, the major change occurs only for the peaks at 1368 and 1395 cm^{-1}, attributed to a decrease in the ionic nitrates. A further temperature increase to 512 K shows the same trend of decreasing ionic nitrates, as well as a slight increase in the size of the peaks at 1305 cm^{-1} and 1555 cm^{-1}, suggesting that the amount of bidentate nitrate species increase to some extent as the ionic nitrates steadily decrease. At temperatures between 512 K and 750 K, both bidentate and ionic nitrates gradually decrease to almost zero.

Similar FTIR experiments were carried out on an NO_2-adsorbed $K_2O(20)/Al_2O_3$ sample to address the question about possible differences in the thermal stability of nitrates between the two relatively high (10 wt% vs. 20 wt%) potassium loadings. As indicated in Fig. 3B, the peaks at 1368 and 1395 cm^{-1} do not change significantly during temperature ramping to 700 K, a result markedly different from the $K_2O(10)/Al_2O_3$ sample. Another interesting feature is the sharpening and possible small growth of the peaks for bidentate nitrate species at 1305 cm^{-1} and 1550 cm^{-1} up to 700 K. Further increase in the temperature above 700 K results in the gradual, and essentially coincident reduction of the FTIR peaks due to the two types of nitrate species, as was also the case for the $K_2O(10)/Al_2O_3$ sample. Still, we note the primary difference between the behavior of these two samples is that the temperature where both nitrate species begin to decrease is shifted to higher temperature (from 512 K to 700 K) when the loading of potassium increases from 10 to 20 wt%. Thus, the formed KNO_3 species on the $K_2O(20)/Al_2O_3$ sample are more thermally stable than the ones on $K_2O(10)/Al_2O_3$, even though the KNO_3 species initially formed on both samples seem to be essentially the same as indicated by the FTIR spectroscopy results.

3.2. TPD on NO_2 pre-adsorbed K_2O/Al_2O_3 samples

As explained above, FTIR results (Fig. 3) obtained during temperature ramping indicates an enhanced thermal stability for the nitrate species formed on the sample at K loadings of 20 wt%. In order to further investigate the thermal stability of the nitrate species on K_2O/Al_2O_3 with various K loadings, TPD experiments were performed after NO_2 adsorption at room temperature on the samples with procedures essentially identical to those used in the FTIR experiments. The main difference is the base pressure (vacuum vs. 1 atm of He) during the decomposition of nitrates. NO_2 TPD curves from $K_2O(x; 2, 5, 10$ and 20 wt%$)/Al_2O_3$ samples are illustrated in Fig. 4. Because a chemiluminescence NO_x analyzer was used in these NO_2 TPD experiments, the desorption of NO (Fig. 4A) and NO_2 (Fig. 4B) could be separately distinguished. Note that for the case of BaO/Al_2O_3 samples, the NO_2 TPD results showed the desorption of NO_2 at 750 K and NO at 820 K, due to the decomposition of surface and bulk barium nitrates, respectively, as evidenced by a combination of FTIR, ^{15}N NMR and NO_2 TPD results [13]. Furthermore, TEM and XRD results showed that higher Ba loadings led to increased amounts of bulk type $Ba(NO_3)_2$.

Upon NO_2 saturation of the $K_2O(2)/Al_2O_3$ sample at room temperature, the temperature was ramped to 900 K while obtaining NO and NO_2 evolution. The NO_2 and NO desorption features around 740 K and 830 K, respectively, are very similar to NO_2 TPD from BaO/Al_2O_3 samples at barium loadings of less than 8 wt%. With increasing K loading to 5 wt%, the ratio of NO to NO_2 desorbed increased, and this trend continues as K loadings increase to 10 and 20 wt%. Significantly, $K_2O(20)/Al_2O_3$ desorbs mostly NO during TPD at quite high (>900 K) temperatures, consistent with the FTIR results (Fig. 3B) showing more thermally stable nitrates for this catalyst. Using a combination of the FTIR and NO_2 TPD results, we suggest that the dominant desorption of NO at higher temperatures is most likely explained by the decomposition of more thermally stable nitrate species in bulk-like K_2O particles that are present at high loadings, while a finely dispersed, "surface" type KNO_3 phase is formed at low coverage. Again, this result for K-based LNTs is quite similar to what has been previously observed for Ba-based catalysts.

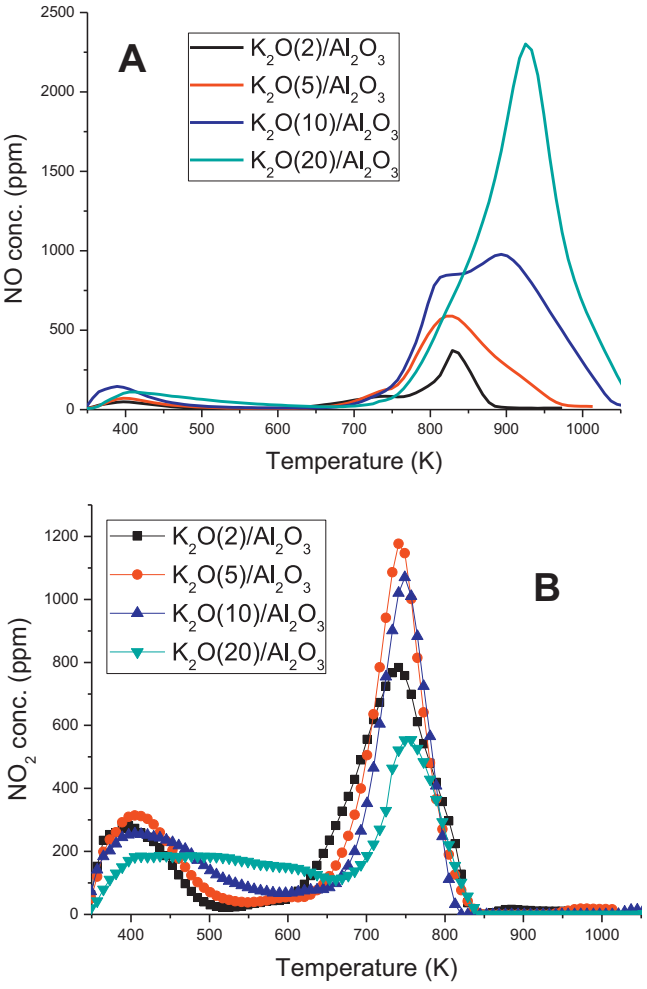

Fig. 4. Temperature programmed desorption (TPD) after room temperature adsorption of NO_2 over $K_2O(x)/Al_2O_3$ samples, where x is the K_2O loading of 2, 5, 10 and 20 wt%. (A) NO and (B) NO_2 evolution.

3.3. NO_x storage-reduction performance on Pt–K_2O/Al_2O_3 catalysts

So far we have discussed the interesting effects of K loading on the formation and decomposition of nitrates formed on NO_2 pre-adsorbed K_2O/Al_2O_3. It should be pointed out that the IR and NO_2 TPD results deal with the thermal decomposition of nitrate species, not their removal by reductants as performed in the NO_x storage-reduction process. Having demonstrated a close relationship between thermal decomposition and the reduction of nitrates in the case of Ba-based LNT materials [23], it is appropriate to consider whether this is also the case for K-based NSR catalysts. In particular, an important question we would like to address next is how the nitrate formation/decomposition behavior of K_2O/Al_2O_3 as a function of K loading is related to the NO_x storage and reduction performance of Pt–K_2O/Al_2O_3 NSR catalysts.

For example, Fig. 5 shows typical NO_x uptake curves using a Pt(2%)–$K_2O(20)/Al_2O_3$ sample obtained at 573 K and 723 K. After introducing 20 lean and rich pulses (50 s/10 s), NO_x uptake was measured during a final lean phase. The uptake amounts were calculated by integrating the amount of NO_x stored up until the time that NO_x concentrations reach 20% (i.e. 30 ppm) of their inlet concentration as marked in the filled area in Fig. 5 for reaction at 573 K. Uptake values obtained in this way emphasize more practically relevant initial stage NO_x storage capacities, rather than full NO_x storage capacities. Similar NO_x uptake curves to those shown in

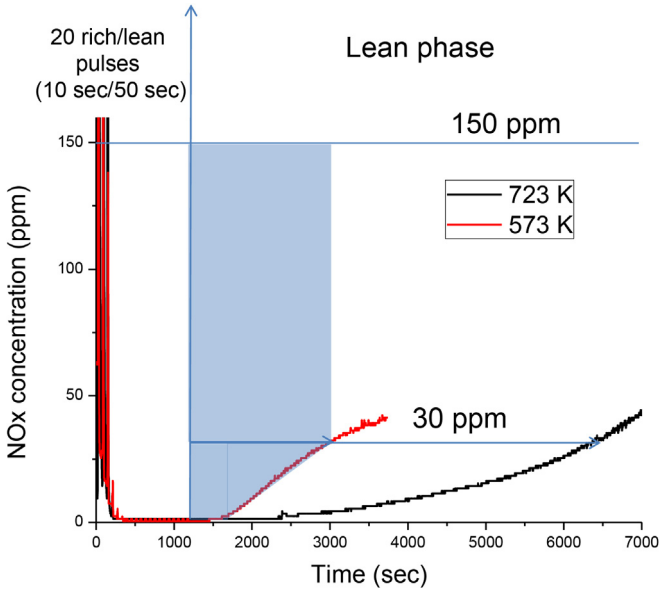

Fig. 5. Raw NO_x uptake curves including 20 rich/lean cycles obtained at 573 K and 723 K for Pt–$K_2O(20)/Al_2O_3$ sample.

Fig. 5 were obtained at a variety of temperatures for NSR catalyst samples that contain K loadings of 5 to 30%.

Fig. 6 shows the amount of NO_x uptake for fresh Pt–K_2O/Al_2O_3 samples with various K loadings over the temperature range from 523 K to 773 K. For the 5 wt% of K-loaded catalyst, maximum NO_x storage capacity was observed at around 573 K (T_{max}). When K loadings doubled (i.e. 10 wt%), the amount of NO_x uptake increased by about 30% over the whole temperature range, without changing the T_{max} at 573 K. As the K loadings increased from 10 wt% to 14 wt%, however, the T_{max} shifted significantly to 673 K in addition to a large increase in the overall NO_x uptake. Further increase in the K loading to 20 wt% gives rise to an even higher (723 K) maximum NO_x uptake temperature. Moreover, the amount of NO_x uptake at T_{max} for the 20 wt% catalyst (723 K) is more than three times that at T_{max} (573 K) of the Pt(2%)–$K_2O(10)/Al_2O_3$ sample. At still higher K loadings of 30 wt%, the overall NO_x storage activity decreases significantly, especially at temperatures below T_{max} (723 K) for this catalyst. This drop in NO_x storage activity for the sample with

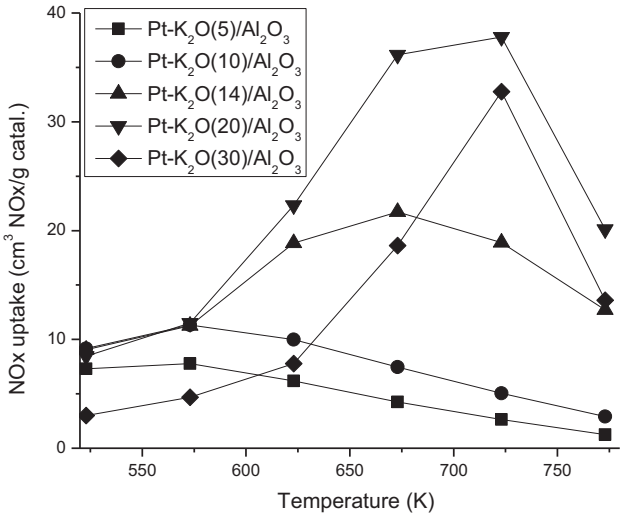

Fig. 6. Changes in the NO_x uptake amounts for Pt–$K_2O(x)/Al_2O_3$ samples, where x is 5, 10, 14, 20 and 30 wt%.

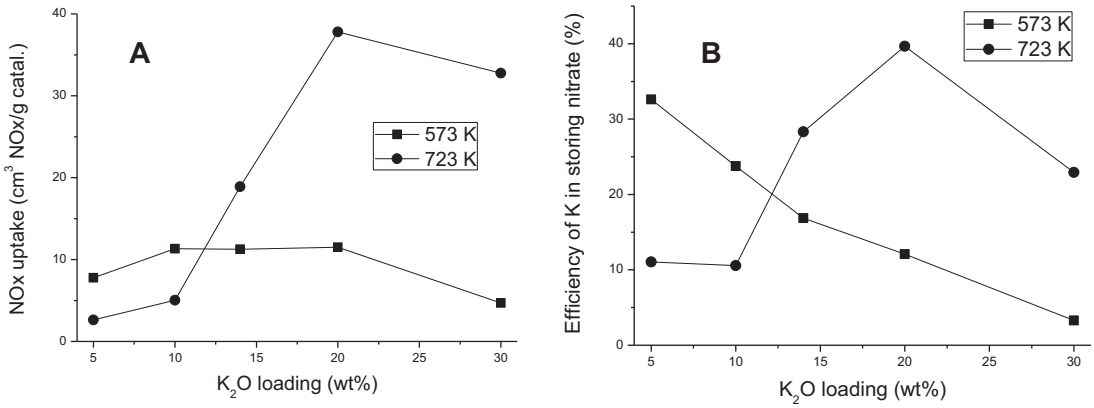

Fig. 7. Changes in the NO_x uptake (A) and the efficiency of K in NO_x storage (B) at 573 K and 723 K as a function of K_2O loadings.

30 wt% K loading can likely be attributed to a partial covering of Pt with K, resulting in a lowering of NO oxidation rates.

The shift toward higher maximum NO_x uptake temperatures (from 573 K to 723 K) with K loading has also been observed for Pt–K_2O/$MgAl_2O_4$ catalysts as K loadings increase from 5 wt% to 10 wt% [16]. However, for the $MgAl_2O_4$-supported catalysts, the amount of NO_x uptake (between 13 and 15 cm^3 NO_x/gram of catalyst) at T_{max} hardly changes in those temperature ranges. In case of the Al_2O_3-supported Pt–K_2O samples, a similar temperature shift from 573 K to 723 K was observed with increasing K loading from 10 wt% to 20 wt%. More importantly, NO_x uptake is about three times higher (38 cm^3 NO_x/gram of catalyst) on the Pt–$K_2O(20)/Al_2O_3$ sample.

Another interesting way to look at the performance data is to plot NO_x uptakes as a function of K_2O loading as is done in Fig. 7A for two representative temperatures (573 K and 723 K). At 573 K, the amounts of NO_x uptake hardly changes with increases in K_2O loading. However, note the significant dependence of NO_x uptake on K_2O loading when performance is tested at 723 K, with the especially notable jump in NO_x uptake at loadings between 10 wt% and 20 wt%. On the other hand, Pt–$K_2O(30)/Al_2O_3$ has somewhat lower NO_x uptake than Pt–$K_2O(20)/Al_2O_3$ at both temperatures plotted in Fig. 7A.

From this data, we can also determine how much of the K takes part in NO_x uptake. The efficiencies of K species for storing nitrate for the various catalysts studied here were calculated from the ratio of the number of stored NO_x molecules to the number of K atoms. These efficiencies are compared at 573 K and 723 K as a function of K_2O loading in Fig. 7B. For example, at low temperature (573 K), 33% of K participates in storing NO_x for the Pt–$K_2O(5)/Al_2O_3$ catalyst. As the amount of K_2O increases to 30 wt%, this efficiency of K use monotonically decreases, there being only a limited portion of K utilized for NO_x storage at high K loading. In contrast, K efficiencies improve significantly at higher temperature (723 K) for K loadings above 10 wt%. Indeed, almost 40% of the K is used to store NO_x at a K loading of 20 wt% during the 'initial' phase of NO_x storage (i.e., up to a breakthrough of 20% of the inlet NO_x concentration). This is even higher than the efficiencies recently reported by Shen et al. where a maximum K-use efficiency of 33 wt% was found for K-titanate nanobelt supported Pt–K NSR catalysts [24]. As for the alumina-supported NSR catalysts (described here) at higher temperatures, efficiencies of the K-titanate-supported materials increased with K loading [24]. Note that this behavior is completely different than Pt–BaO/Al_2O_3 catalysts, where a monotonic decrease in the overall efficiency of Ba use with increasing Ba loading was consistently observed [25].

The results reported here provide important new insights regarding the behavior of K-based NSR catalysts by focusing on a characterization of their NO_x storage properties as a function of K loading. In particular, maximum NO_x storage performance (38 cm^3/gm-catalyst) and the superior efficiency of K use (40%) were observed at a K loading of 20 wt% when measured at the temperature of maximum activity (T_{max} = 723 K), demonstrating significantly improved high temperature performance relative to Ba-based NSR catalysts. In this contribution, important durability issues such as the mobility of K, thermal stability and sensitivity to SO_2 poisoning are not covered, but these issues will need to be addressed in the near future before more practical application of this class of NSR catalysts can be realized.

4. Conclusions

Effects of potassium loading on nitrate formation/decomposition processes over K_2O/Al_2O_3 samples, and on NO_x storage performance over Pt–K_2O/Al_2O_3 catalysts were investigated by a combination of FTIR spectroscopy, NO_2 TPD, and activity measurements. FTIR results demonstrate that ionic and bidentite nitrates species are present and that the ratio of the former to the latter increases with increasing potassium loading up to 10 wt%, after which the ratio stayed nearly constant. While NO_2 pre-adsorbed $K_2O(10)/Al_2O_3$ and $K_2O(20)/Al_2O_3$ samples are hardly differentiated spectroscopically, the latter has significantly more thermally stable nitrate species, as demonstrated by the temperature dependence of the FTIR spectra and the NO_2 TPD results. The temperature of maximum NO_x uptake (T_{max}) is 573 K up to potassium loadings of 10 wt%. T_{max} then gradually shifts from 573 K to 723 K as the potassium loading increases from 10 wt% to 20 wt%. Moreover, the amount of NO_x uptake at T_{max} increases more than three times, indicating that efficiency of the K for storing NO_x is enhanced considerably at higher temperature, in good agreement with our NO_2 TPD and FTIR results. These combined characterization and performance measurements provide interesting contrasts in the effects of potassium loading on nitrate formation and decomposition processes in comparison to Ba-based NSR catalysts, and they demonstrate the potential for high temperature NSR applications for Pt–K_2O/Al_2O_3 materials.

Acknowledgements

Financial support was provided by the U.S. Department of Energy (DOE), Office of Energy Efficiency and Renewable Energy, Vehicle Technologies Program. The research was performed in the Environmental Molecular Sciences Laboratory (EMSL), a national scientific user facility sponsored by the U.S. DOE's Office of Biological and Environmental Research, and located at Pacific Northwest

National Laboratory (PNNL). PNNL is a multi-program national laboratory operated for the U.S. Department of Energy by Battelle. Prof. Do Heui Kim acknowledges the partial support of Research Settlement Fund for the new faculty of Seoul National University.

References

[1] Z.M. Liu, S.I. Woo, Catalysis Reviews – Science and Engineering 48 (2006) 43–89.
[2] S. Roy, A. Baiker, Chemical Reviews 109 (2009) 4054–4091.
[3] R. Buchel, R. Strobel, A. Baiker, S.E. Pratsinis, Topics in Catalysis 52 (2009) 1799–1802.
[4] L. Castoldi, L. Lietti, P. Forzatti, S. Morandi, G. Ghiotti, F. Vindigni, Journal of Catalysis 276 (2010) 335–350.
[5] N. Takahashi, S. Matsunaga, T. Tanaka, H. Sobukawa, H. Shinjoh, Applied Catalysis B – Environmental 77 (2007) 73–78.
[6] M. Takeuchi, S. Matsumoto, Topics in Catalysis 28 (2004) 151–156.
[7] J.R. Theis, E. Gularl, Applied Catalysis B – Environmental 74 (2007) 40–52.
[8] T.J. Toops, D.B. Smith, W.S. Epling, J.E. Parks, W.P. Partridge, Applied Catalysis B – Environmental 58 (2005) 255–264.
[9] T.J. Toops, D.B. Smith, W.P. Partridge, Applied Catalysis B – Environmental 58 (2005) 245–254.
[10] L. Castoldi, L. Lietti, R. Bonzi, N. Artioli, P. Forzatti, S. Morandi, G. Ghiotti, Journal of Physical Chemistry C 115 (2011) 1277–1286.
[11] T. Montanari, R. Matarrese, N. Artioli, G. Busca, Applied Catalysis B – Environmental 105 (2011) 15–23.
[12] S.J. Park, H.A. Ahn, I.J. Heo, I.S. Nam, J.H. Lee, Y.K. Youn, H.J. Kim, Topics in Catalysis 53 (2010) 57–63.
[13] J. Szanyi, J.H. Kwak, D.H. Kim, S.D. Burton, C.H.F. Peden, Journal of Physical Chemistry B 109 (2005) 27–29.
[14] F. Frola, M. Manzoli, F. Prinetto, G. Ghiotti, L. Castoldi, L. Lietti, Journal of Physical Chemistry C 112 (2008) 12869–12878.
[15] L. Castoldi, I. Nova, L. Lietti, P. Forzatti, Catalysis Today 96 (2004) 43–52.
[16] D.H. Kim, K. Mudiyanselage, J. Szanyi, H. Zhu, J.H. Kwak, C.H.F. Peden, Catalysis Today 184 (2012) 2–7.
[17] F. Prinetto, M. Manzoli, S. Morandi, F. Frola, G. Ghiotti, L. Castoldi, L. Lietti, P. Forzatti, Journal of Physical Chemistry C 114 (2010) 1127–1138.
[18] T. Montanari, L. Castoldi, L. Lietti, G. Busca, Applied Catalysis A – General 400 (2011) 61–69.
[19] T. Lesage, J. Saussey, S. Malo, M. Hervieu, C. Hedouin, G. Blanchard, M. Daturi, Applied Catalysis B – Environmental 72 (2007) 166–177.
[20] J. Szanyi, J.H. Kwak, R.J. Chimentao, C.H.F. Peden, Journal of Physical Chemistry C 111 (2007) 2661–2669.
[21] J.H. Kwak, D.H. Mei, C.W. Yi, D.H. Kim, C.H.F. Peden, L.F. Allard, J. Szanyi, Journal of Catalysis 261 (2009) 17–22.
[22] J.H. Kwak, J.Z. Hu, D.H. Kim, J. Szanyi, C.H.F. Peden, Journal of Catalysis 251 (2007) 189–194.
[23] T. Szailer, J.H. Kwak, D.H. Kim, J.C. Hanson, C.H.F. Peden, J. Szanyi, Journal of Catalysis 239 (2006) 51–64.
[24] W.H. Shen, A. Nitta, Z. Chen, T. Eda, A. Yoshida, S. Naito, Journal of Catalysis 280 (2011) 161–167.
[25] J.H. Kwak, D.H. Kim, T. Szailer, C.H.F. Peden, J. Szanyi, Catalysis Letters 111 (2006) 119–126.